Available online at www.sciencedirect.com

SciVerse ScienceDirect

Ceramics International 39 (2013) 2197–2206

CERAMICS INTERNATIONAL

www.elsevier.com/locate/ceramint

Review paper

Hydroxyapatite nanocomposites: Synthesis, sintering and mechanical properties

M. Aminzare[a], A. Eskandari[b,*], M.H. Baroonian[d], A. Berenov[c], Z. Razavi Hesabi[b], M. Taheri[a], S.K. Sadrnezhaad[e]

[a]Department of Materials and Metallurgical Engineering, Iran University of Science and Technology, Tehran, Iran
[b]Department of Materials Engineering, Science and Research branch, Islamic Azad University, Tehran, Iran
[c]Department of Materials, Imperial College London, Exhibition Road, London SW72AZ, UK
[d]Materials and Energy Research Center (MERC), Tehran, Iran
[e]Department of Materials Science and Engineering, Sharif University of Technology, Tehran, Iran

Received 10 June 2012; received in revised form 5 September 2012; accepted 6 September 2012
Available online 13 September 2012

Abstract

Two different hydroxyapatite based composites reinforced by oxide ceramic (20 wt%) nano crystals were synthesized by high-energy ball milling and sintered by pressure less technique. Alumina and titania nanoparticles as secondary phases improved densification and mechanical behavior of apatite and postponed its decomposition to the tricalcium phosphate (TCP) phases at elevated temperatures. Increasing the relative density of apatite using nano reinforcements leads to enhance the bending strength by more than 40% and 27% (as compared to the pure HA) and increase the hardness from 2.52 to 5.12 (Al_2O_3 composite) and 4.21 (TiO_2 addition) GPa, respectively. Transmission electron microscopy (TEM), scanning electron microscopy (SEM) and X-ray diffraction spectroscopy were employed to study morphologies, fracture surfaces and phase compositions, respectively. The morphological study and micro structural analysis confirm the X-ray diffraction and relative density diagrams.

Keywords: A. Sintering; B. Nanocomposites; C. Mechanical properties; Hydroxyapatite

Contents

1. Introduction

Several paradigm shifts have taken place in different areas such as electronics, robotics, medicine and surgery by the advent of nanomaterials. To some extent, the field of

*Corresponding author. Tel.: +98 912 2388082; fax: +98 21 77240291.
E-mail addresses: arvin.eskandari@yahoo.com, arvin.eskandari86@gmail.com (A. Eskandari).

0272-8842/$ - see front matter © 2012 Elsevier Ltd and Techna Group S.r.l. All rights reserved.
http://dx.doi.org/10.1016/j.ceramint.2012.09.023

medicine and surgery is the most important area because it is related to human's health. In this case, biomaterials play a very important role. Among different categories of biomaterials, bioactive ceramics such as hydroxyapatite are attractive candidates for body's hard tissues replacement [1–4]. Hydroxyapatite (HA, $Ca_{10}(PO_4)_6(OH)_2$) has been widely used as a bulk implant material in non-load bearing areas of the body [5]. Although HA has excellent biocompatibility properties, it is limited in use due to its low strength and brittle nature [6–8]. The main reason of this loss in mechanical properties of HA is decomposition of HA into some calcium phosphate phases such as tricalcium phosphate (TCP) and even tetra-calcium phosphate (TTCP) [9]. Calcium phosphate phases are brittle and have weaker strength. Different techniques have been tried to improve strength and fracture toughness of HA (toughness of pure HA < 1 MPa $m^{1/2}$) [10], such as making composites and using different pressing/sintering methods like underwater shock compaction [10] hot press sintering [3], microwave [5] and spark plasma sintering process [11,12].

Beside the advanced processing routes, bioinert polymer or ceramic materials as reinforcing agents in different forms like whiskers, platelets, fibers and particles have been employed to improve the mechanical properties of HA [13–16]. Moreover, another issue could enhance mechanical properties of apatite is decreasing the grain size, which is well known as Hall–Petch equation [17]. In fact, nanocrystallinity is a key factor for improvement of sinterability and enhancement of compacted specimen behavior owning to high energy and high interface density which are stored in the interfaces of ultrafine grained structures. However, the tendency of nanopowders to agglomeration leads to create some problems in shaping of bodies and there are still challenges in this area. Some effort such as high energy ball milling have been used to overcome/decrease the agglomeration effects [12,18]. The large surface area often dominates the properties of the powders and enhances mechanical, chemical and physical properties, significantly, of the material resulting in interesting and sometimes unexpected behavior of nanoparticles. Nanocrystalline powders of apatite composites can be sintered into well-built osteointegrative ceramic specimens [19].

It has been reported that alumina and titania particles are the best choices for making composite with HA due to their good mechanical properties and bio inertness [1,3,9,15]. As an illustration, Viswanath and Ravishankar [15] have studied the interfacial reactions in hydroxyapatite/alumina nanocomposite. Their work showed that alumina completely reacted with hydroxyapatite and formed alumina-rich calcium aluminates and TCP phases at relatively low temperatures (1000 °C). In contrast, Xihua et al. [3] reported that by introducing diapsoid/alumina and hot pressing the composites under 20 MPa in N_2 atmosphere at 1320 °C, the decomposition of HA was not observed. Que et al. [11] reported that the addition of titania into HA has a major effect on the HA structure and enhanced HA properties. Moreover, because of the introduction of secondary phases, the phase changes in the composites at higher sintering temperatures could take place. Application of the expensive materials processing techniques (e.g. spark plasma sintering) could improve the mechanical properties and bio activity, but the decomposition of HA at 1200 °C results in drastic decreasing the strength of composites. Some attempts have been done to prevent the decomposition. Nath et al. [2], for instance, have tried to inhibit the decomposition reaction of HA into calcium phosphate phases by making HA-Mulite system. Nevertheless, in their study decomposition of HA composites at 1350 °C results in deterioration of the mechanical strength.

The purpose of this work is to study the applicability of a newly devised biomimetic synthesizing technique for the production of the nanocrystalline needle-like apatite powder and subsequent preparation of nanocomposite by high-energy ball milling in order to obtain highly dense objects with desired mechanical properties. The effects of alumina and titania nanoparticles on microstructure, phase decomposition and mechanical properties of the product have also been investigated.

2. Experimental procedure

In the previous study [20], we synthesized the apatite nanocrystals via biomimetic method. In summary, the mixture were composed of acidic calcium phosphate (Merck, 2146) mixed with basic TTCP at 1/1molar ratio and 6 wt% disodium hydrogen phosphate dissolved in distilled water. The solid content of the mixture was 3 g/ml. The hardened paste was maintained in simulated body fluid (SBF) for 7 days. After this period, the material was removed from the SBF, washed with distilled water, dried at 70 °C and ground to fine powder by a planetary mill.

Nanocrystalline alumina powder with the average particle size of 50 nm (Sigma(Aldrich, purity > 99.99%) was used as a secondary phase. Fig. 1 shows X-ray pattern of as-received alumina nanopowder which shows the alpha structure as a predominant phase. To compare the effect of strengthening phases, TiO_2 nanopowder (P25, Degussa Co., Frankfurt, Germany) with a particle size ranging from 11 to 27 nm was employed. TiO_2 powder consisted of 77% anatase and 23% rutile phases. Alumina and titania nanopowders was first mixed with HA nanopowder to obtain 20 wt% mixtures of nanopowders with HA. Powder mixtures were milled in a polymeric ball mill at the speed of 400 rpm, and the weight ratio of ball-to-powder was 10:1. The mixed powders were placed in a cylindrical steel die with 10 mm diameter and pressed uniaxially at 150 MPa.

Non-isothermal sintering was performed upon heating with the rate of 5 °C/min to 1400 °C followed by cooling in an electrical furnace naturally. Sinterability of the compacted powders was determined by bending stresses, Vickers hardness and fractional density measurements.

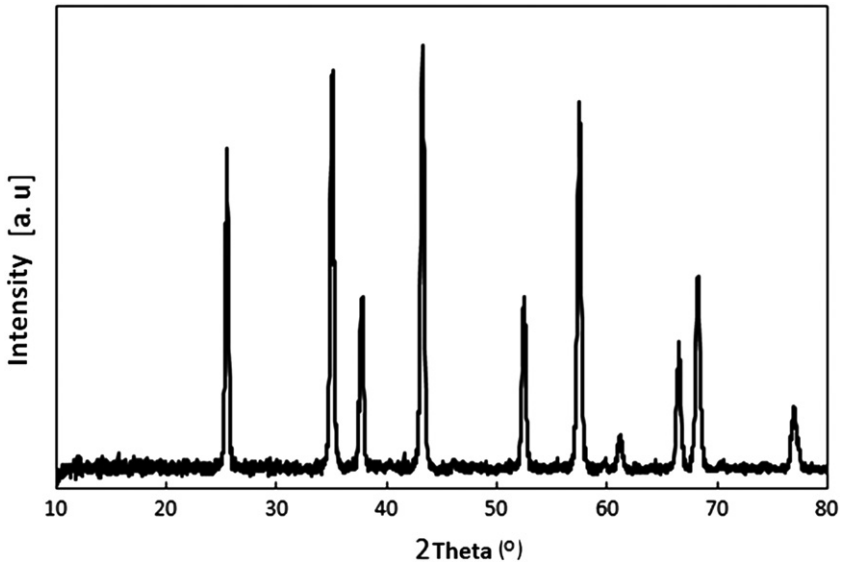

Fig. 1. X-ray pattern of as-received alumina nanopowder.

The values of bending stress were determined by Zwik/Roell machine from 3-point bending test using loading rate of 0.5 mm/min. Water displacement (Archimedes method) was used to measure the densities of the sintered specimens. Vickers hardness was measured by indentation at load of 500 g and dwell time of 20 s. At least three sample sizes were used to determine the average density, hardness and bending strength corresponding to each data point. Vickers impressions were carried through the surfaces of each one of the samples, which already were polished. After the diagonal length measurement, the values of the Vickers hardness (GPa) were calculated, by the following equation [21]:

$$HV = 0.0018544\,(P/d^2) \quad (1)$$

where HV, P and d are the Vickers hardness, the applied load and the arithmetic mean of the two diagonal lengths (mm), respectively. X-ray diffraction (German Unisantis (XMD-300) equipped with monochromatized Cu-Kα1 (1.5418 A°) radiation determined structure and phase composition. The fracture surfaces were observed with a Cambridge scanning electron microscope (SEM) operating at 25 kV.

3. Results and discussion

3.1. Sinterability and phase composition

The morphology of the biomimetically produced nanocrystalline hydroxyapatite has been analyzed by TEM (Fig. 2). The average particle size is around ~50 nm in diameter. Needle-like morphology of the nano hydroxyapatite (nHA) crystals with the aspect ratio of 3 has been attributed to the growth along the [0001] direction, according to some authors [22].

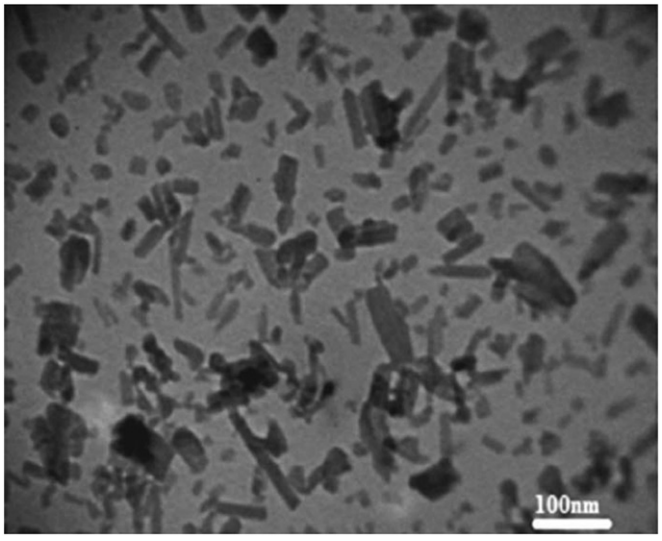

Fig. 2. TEM micrograph of the as-synthesized nanocrystalline hydroxyapatite sample.

To study the phase stability of pure nHA compacts, X-ray diffraction of green and sintered samples was performed (Fig. 3). It is obvious that the pure hydroxyapatite of as-synthesized sample is transformed partially to TCP phase (JCPDS ♯ 029–0359) at 1300 °C. The effect of TCP phase on the specimen properties is clarified in Table 1 which presents the relative densities and mechanical behavior of sintered nHA compacts in the range of 1200–1300 °C. Accordingly, the densification occurred which resulted in increasing the mechanical strengths when annealed up to 1250 °C. It is reported that pure hydroxyapatite which was prepared by wet chemical approach and spark plasma sintered, decompose to the TCP and TTCP phases above 1100 °C [11]. Smaller values of bending strength (57.4 MPa) of hydroxyapatite specimens synthesized by similar method were reported by other

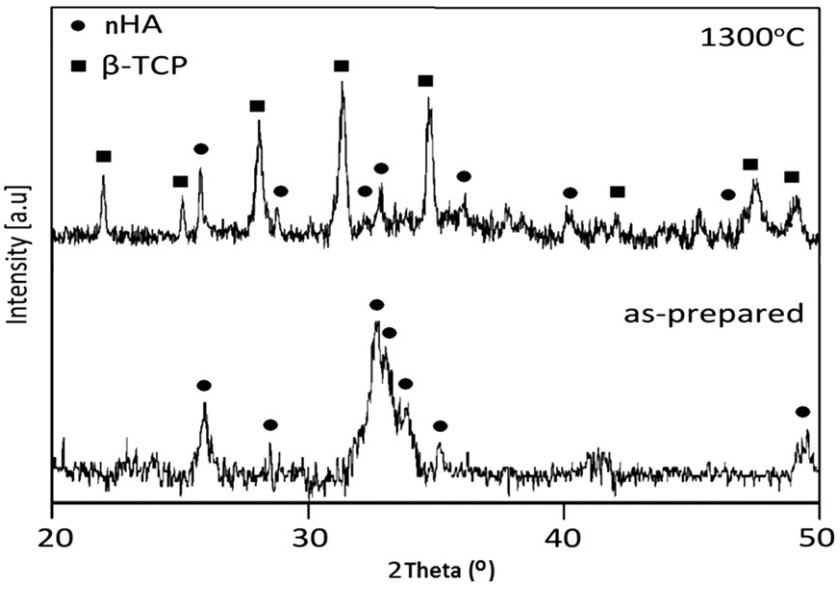

Fig. 3. The X-ray pattern of nano crystalline hydroxyapatite (as-synthesized and sintered at 1300 °C) [20]. (For interpretation of the references to color in this figure caption, the reader is referred to the web version of this article.)

Table 1
Relative density and mechanical properties of hydroxyapatite nano crystals sintered at 1200–1300 °C.

Sintering temperature (°C)	Relative density (%)	Bending strength(Mpa)	Hardness (Gpa)
1200	77	49	2.1
1250	88	61	2.53
1300	82	28	2.1

investigators [23]. Further annealing (1300 °C) resulted in decreasing the relative density of specimens. Therefore, a significant drop in bending strength as well as hardness was found. Decreasing of density and the deterioration of mechanical properties are attributed to the decomposition of nHA at 1300 °C and the formation of TCP phase. In other word, the densification ($T < 1250$ °C) and decomposition ($T > 1250$ °C) are the main phenomena during sintering process. Note that TCP is a typical biomaterial with excellent biocompatibility and osteoconductivity, by which the formation of new bone tissue is accelerated when these materials are implanted into the body [10]. TCP is fragile bioceramic and consequently cannot be used on their own as major load-bearing implants in the human body[14].

Fig. 4 shows the XRD pattern of nHA/Al_2O_3nano composite which was prepared by mechanical milling. All the peaks were assigned to nHA and alumina phases and no TCP phase were observed. Another reinforcement phase was TiO_2 nanoparticles. Fig. 5 shows the X-ray pattern of nHA/titania nanocomposite.

To investigate the effect of the reinforcements as secondary phases on the sintering behavior and mechanical properties of nanocomposite, the green bodies of composites were sintered up to 1400 °C. Fig. 6 shows the relative densities of nanocomposites in comparison with biomimetic hydroxyapatite. It can be seen from the this figure that the measured densities of the nHA samples and the nHA/TiO_2 composites increase gradually by increasing the sintering temperature up to maximum value and then starting to decrease with the further increasing in the sintering temperature. According to the Fig. 6 the three different sintering stages can be distinguished: (i) slight increase of the fractional density from 66% to 71% between 950 and 1150 °C, (ii) interconnection of the apatite particles during rapid sintering stage occurring between 1150 and 1250 °C which yields maximum density of the sintered specimen, and (iii) necking in the first stage sintered specimen as described by the previous investigation [24]. After that, the large decrease in densification is appeared for pure nHA while the density of nanocomposite continued to increase up to 1300 °C. The reduction of the nHA density can be attributed to the decomposition that results in the formation of calcium phosphates and water through the following reaction:

$$Ca_{10}(PO_4)_6(OH)_2 \rightarrow Ca4P_2O_9 + 2Ca_3(PO_4)_2 + H_2O \quad (2)$$

The same trend for nHA/TiO_2 nanocomposite samples can be observed in this figure. It can also be monitored that the density values of the titania and alumina composites sintered at different temperatures are smaller than those of the pure nHA samples before 1250 °C. The main reason for smaller values of relative densities of nanocomposites is lower green densities due to the existence of secondary phases which could inhibit the pressure flow during the compaction. Despite the fact that the decomposition temperature of nHA should be the same in both specimens (starting at T, $1250 < T < 1300$ °C), addition of 20 wt% TiO_2 or alumina nanopowders affected the

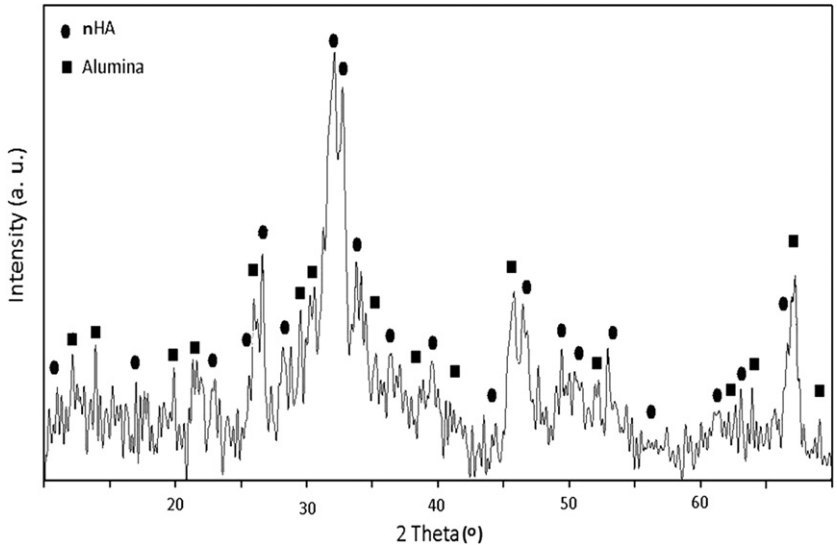

Fig. 4. XRD pattern of as-synthesis nHA/Al_2O_3 nanocomposite.

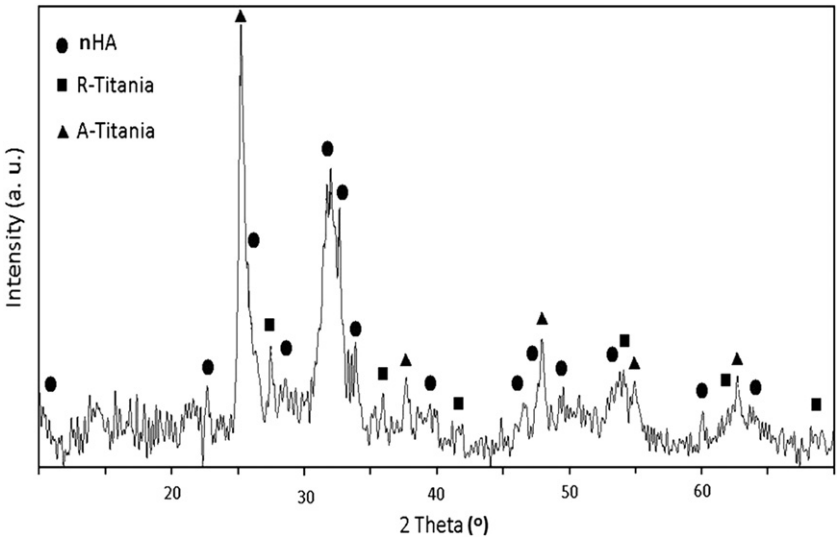

Fig. 5. XRD pattern of nHA/TiO_2nanocomposite before sintering process.

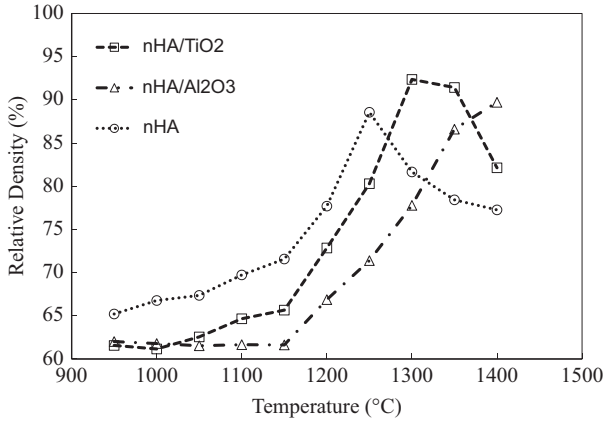

Fig. 6. Changes in relative density with temperature through sintering process.

maximum density value and the decomposition temperature of nHA composites. As seen, in nHA/TiO_2 nanocomposite the decomposition process is observed at higher temperatures which results in the enhancement of the higher density (~93% theoretical relative density, TD, at 1300 °C). Indeed, in the competition between densification and decomposition processes, the densification is the main phenomena before optimum-sintering temperature (1300 °C) is reached and followed by the formation of TCP phase affecting the density and also mechanical properties.

Similarly, it is reported that by using fine 3YSZ as second phase, HA/3YSZ nanocomposite decomposition (TCP phase formation) was hindered from 1050 °C to 1150 °C comparative to pure hydroxyapatite by high frequency induction heat sintering [25].

X-ray diffraction pattern of sintered nHA/TiO_2 composite is illustrated in Fig. 7. Peaks belonging to the nHA and TiO_2 as major phases were observed. One can observe the TCP, CaO and $CaTiO_3$ phases, additionally. It is notable that anatase-rutile phase transformation is also occurred at relatively low temperature (~650 °C) [26]. The presence of α-TCP was detected for the entire range of sintering temperatures (from 1300 to 1400 °C). The following equation can be used for the chemical reaction between nHA and titania

$$Ca_{10}(PO_4)_6(OH)_2 + TiO_2 \rightarrow 3Ca_3(PO_4)_6(TCP) + CaTiO_3 + H_2O\uparrow \quad (3)$$

Alumina reinforced composite has shown lower rate of densification (Fig. 6). The maximum value of relative density (TD%) is ~90% by sintering at 1400 °C. Moreover, no declining in density value was observed above 1300 °C in sintering regime. The high sintering density would come from the particle size of Al_2O_3 powder which has ultrafine particle sizes with surface area higher than TiO_2 particles. XRD pattern of nHA/Alumina samples at 1350 °C is shown in Fig. 8. The sintered pellet contains several phases such as CaO, calcium aluminate phases and α-TCP as expected according to Eq. (3). In the presence of Al_2O_3, the highest value of obtainable density increased 1.3% in respect to pure nHA. Interestingly, increasing the density and decomposition of matrix occurred, simultaneously. The density enhancement of composites reveals that the densification process is succeeded. Based on the results, the decomposition could not affect the relative density even by sintering at 1400 °C. We propose added alumina nanoparticles had changed the reaction decomposition of nHAs into another, resulting in formation of some types of calcium aluminates through the following reaction:

$$Ca_{10}(PO4)_6(OH)_2 + 6Al_2O_3 \rightarrow CaO.6Al_2O_3 + CaAl_2O_4 + 3Ca_3(PO4)_2 + H_2O \quad (4)$$

The formation and kinetics of calcium aluminates have been well documented in the literature [15]. For instance, the reactions between nHA and alumina in nHA/Alumina nanocomposites studied and reported that nanocrystalline alumina plays important role in the formation of the TCP phase. They suggested that the Ca^{2+} diffuses from hydroxyapatite into alumina lattice to form tricalcium phosphate and calcium aluminates phases at interface.

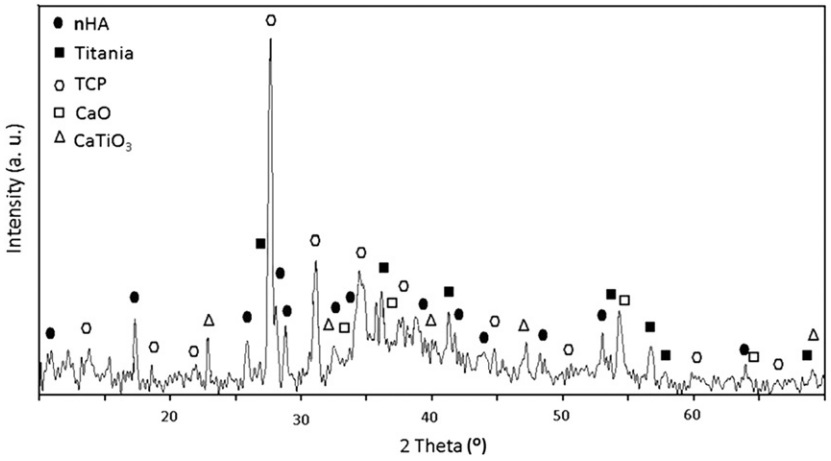

Fig. 7. XRD pattern of nHA/TiO_2 composite sintered at 1350 °C.

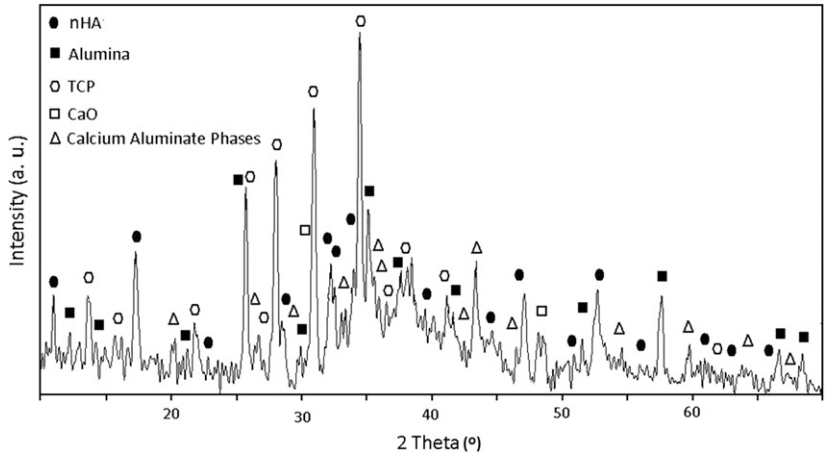

Fig. 8. XRD pattern of nHA/Al_2O_3 composite sintered at 1350 °C.

3.2. Mechanical properties

Al_2O_3 and TiO_2 nanoparticles changed the mechanical behavior of hydroxyapatite remarkably. The effect of the incorporation of reinforcements on bending strength of hydroxyapatite nano crystal as a function of sintering temperature is shown in Fig. 9. Hence the densities and mechanical properties of calcium aluminates ($CaAl_2O_4$, $CaO.6Al_2O_3$) and $CaTiO_3$ are higher than nHA and TCP, the adding of alumina and titania nanopowders resulted in the improvement in densification and have a significant effect on the mechanical behavior of specimens as well. Based on our results, the value of the bending stress increase gradually with the temperature up to 61 MPa (1250 °C), 78 MPa (1300 °C), 85.8 MPa (1400 °C) for pure nHA, nHA/TiO_2 and nHA/Alumina, respectively. Enhancement of the bending strength up to ~27% and ~40% are achieved using TiO_2 and Al_2O_3 nanoparticles, respectively. According to phase transformation and decomposition that were detected (Figs. 7 and 8), with the further increase of the sintering temperature, the TCP and $CaTiO_3$ phases were formed in pure and TiO_2 contained composite. This leads to drastic decrease (about 35%) in bending strength of TiO_2 reinforced nanocomposite. This finding is in agreement with decreasing of the relative density observed after acquiring the maximum value. In general, sintered samples with higher relative density improved mechanical properties.

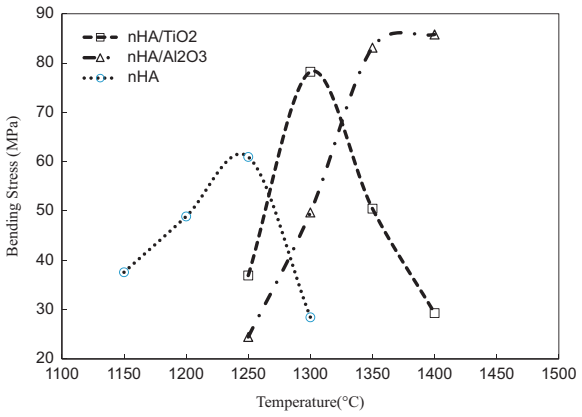

Fig. 9. Bending strength as a function of sintering temperature for pure nHA, nHA/TiO_2 and nHA/Al_2O_3 nanocomposites.

The density of nHA/Alumina samples increased with the temperature. In other words, the aluminate phases exhibit better flexural strength of nanocomposite in comparison with titanate ones at 1350 °C. The maximum bending strength was observed in the sample containing alumina and sintered at 1400 °C. The major value of relative density is for the sample containing titania reinforcing agent and sintered at 1300 °C. Interestingly, the alumina contained sample with lower density as compared to TiO_2, showed greater value of bending strength. It could be speculated that the aluminate phases have better bending behavior than $CaTiO_3$ and the difference originates from the nature of $CaAl_2O_4$ and $CaTiO_3$.

Comparing the microhardness results of the samples heat treated at 1250 up to 1400 °C with those of the nHA prepared at the same temperature, an increase in the microhardness of the samples with the introduction of nanoparticles is verified in Table 2 (SD = standard deviation). The dependence temperatures for the hardness of nanocomposites resembles those of the densification behavior and bending strength. In fact, the hardness of nHA/TiO_2 nanocomposite increases by increasing the sintering temperature and density from 1.62 to 4.21 GPa at 1300 °C. As anticipated, the micro hardness started to decrease owing to decomposition of pure apatite to TCP and $CaTiO_3$ phases and decreasing the relative density. Especially, the value of the hardness decrease to 46% when sintered at 1400 °C. Que et al. [11] reported that the maximum value of hardness of nHA/TiO_2 composite derived by high-energy ball milling and spark plasma sintered at 1100 °C is about 3.45 GPa which is 18% inferior than accounted in our investigation. They believed that the formation of the multi-phases in the composites because of chemical decomposition and mutual reaction between TiO_2 and nHA should contribute to decreasing the density values of the composites. In other research [27], flexure strength and hardness of the HA-10 wt% TiO_2 porous bodies produced by post-sintering hot isostatic pressing (HIP) were 16 MPa and 1 GPa, correspondingly.

However, nHA/Alumina samples sintered below 1300 °C, showed the lower values of hardness in contrast to pure nHA. Further sintering process increases the hardness to 5.12 GPa which is larger than the measured value of pure and TiO_2 contained composite. Xihua et al. [3] prepared HA composite by adding alumina and diopside as reinforcement agents. The hardness of 10 wt% Alumina–88 wt% HA–2 wt% diopside samples hot pressed at 1320 °C and 20 MPa pressure for 6 min was 4.7 GPa. The mechanical

Table 2
Hardness results for pure nHA, alumina and titania containing composites.

Temperature (°C)	Pure nHA		Titania		Alumina	
	Hardness (Gpa)	SD $(GPa)^{0.5}$	Hardness (Gpa)	SD $(GPa)^{0.5}$	Hardness (Gpa)	SD $(GPa)^{0.5}$
1250	2.52	0.09	1.62	0.05	1.03	0.06
1300	2.23	0.11	4.21	0.13	1.87	0.07
1350	–	–	3.77	0.05	4.71	0.1
1400	–	–	3.27	0.08	5.12	0.12

Table 3
Comparison of mechanical strength and hardness of pure nHA, nHA/Al_2O_3 and nHA/TiO_2 nanocomposties with literature.

Materials	Processing details	References	Hardness (Gpa)	Bending strength (MPA)
Pure Hydroxyapatite nanocrystal	Biomimetic synthesizing/ Pressure less sintering	This work	2.53	61
Pure Hydroxyapatite	Precipitation/ Pressure less sintering	[8]	0.48	–
nHA/TiO_2	Biomimetic/Mechanical milling/ Pressure less sintering	This work	4.21	78
nHA/Al_2O_3	Biomimetic/Mechanical milling/ Pressure less sintering	This work	5.12	85.8
HA/Polycaprolactone	Wet precipitation	[13]	0.22	–
HA/TiO_2	High energy milling/ Spark Plasma Sintering(SPS)	[11]	3.45	–
HA/TiO_2	Hot Isostatic Pressing(HIP)	[25]	1	16
HA/diopside/Al_2O_3	Hot Pressing (HP)	[3]	4.7	–
HA/Silver	Biomimetic	[16]		80
HA/nylone-6	Biomimetic	[16]		< 50

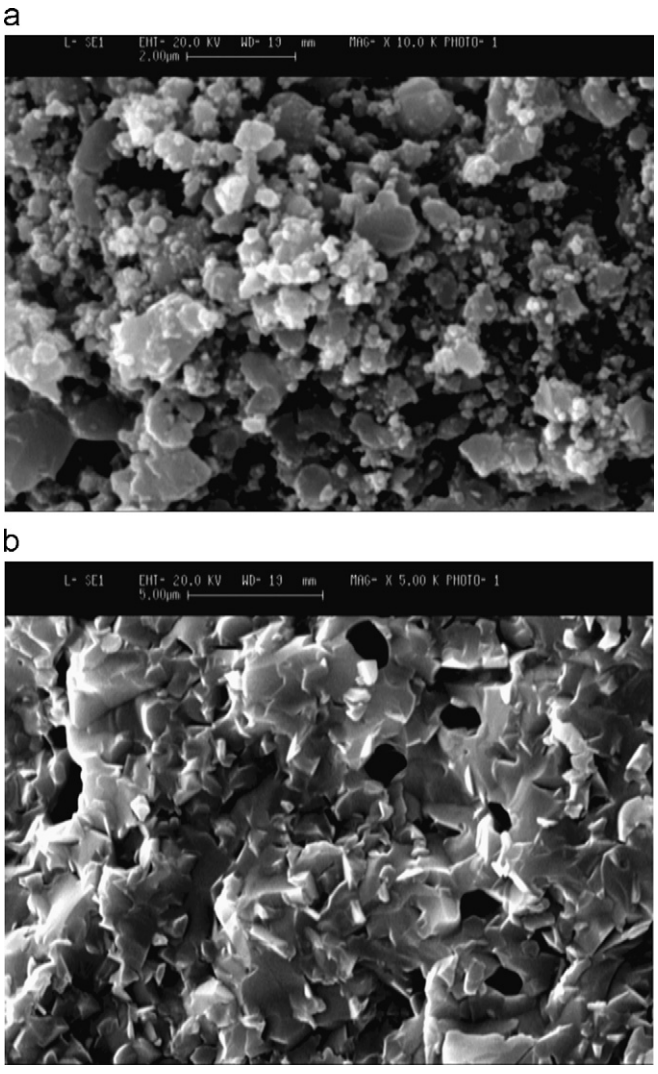

Fig. 10. SEM micrographs of fracture surface of nHA/Al_2O_3 composites sintered at 1250 °C (a) and 1400 °C (b).

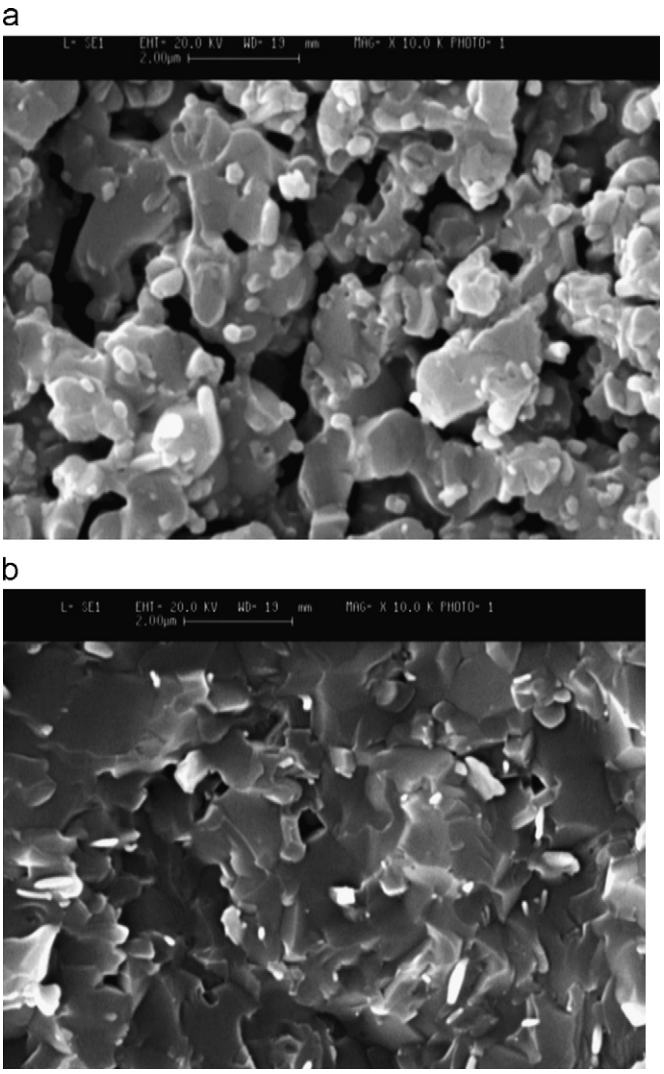

Fig. 11. SEM micrographs of fracture surface of nHA/TiO_2 composites sintered at 1250 °C (a) and 1300 °C (b).

properties of nHA/TiO_2 and nHA/Al_2O_3 were found to have outstanding characteristics comparable to other research which are shown in Table 3.

Fig. 10(a) and (b) shows the scanning electron micrographs of fracture surfaces of hydroxyapatite/alumina nanocomposite after sintering at 1250 °C and 1400 °C, respectively. As seen, denser composite was obtained at higher sintering temperature resulting in enhanced mechanical characteristics. Fractured surface images of nHA/TiO_2 samples sintered at 1250 °C and 1300 °C

pressure less sintering process are shown in Fig. 11(a) and (b), respectively. It appears that the addition of TiO_2 nanoparticles significantly improve sample density and decrease irregular porosity of the specimens. A large number of small pores were detected within grains of nHA/TiO_2 nano composite while, fewer pores can be clearly observed for the samples sintered at 1300 °C which result in enhancing the mechanical properties. Apparently, these results are in good agreement with results of bending strength, hardness and theoretical density measurements which can be used to understand the evolution of the density during the processing.

4. Conclusions

Nano hydroxyapatite particles of ~50 nm diameter were synthesized by a biomimetic method as matrix of composite. Alumina and titania nanoparticles were added to reinforced matrix via high-energy ball milling, successfully. The mixtures were sintered up to 1400 °C in order to study the densification process and evaluation of the mechanical characteristics. As a result, since decomposition of nHA into tricalcium phosphate (TCP) is known to be the main reason for the drop in density and mechanical properties of nHA, added titania and alumina nanopowders will delay the deterioration of the mechanical behavior of nHA from 1250 °C to 1300 °C and 1400 °C, respectively. The enhancement of the bending strength by ~27% and ~40% are achieved using TiO_2 and Al_2O_3 nanoparticles, correspondingly. Increasing the hardness from 2.52 (pure nHA) to 5.12 (alumina added) and 4.27 GPa (titania added) were measured. These improvements originate from the formation of calcium aluminates and calcium titanate phases when alumina and titania used as additives, respectively. Comparative study showed that titania contained composite, however, densified earlier than the one with added alumina. By using nano alumina as a second phase, the flexural strength and hardness enhanced at higher temperature. The SEM images and micro structural analysis confirm the X-ray diffraction and relative density diagrams.

Acknowledgments

The authors gratefully acknowledge Dr. Parvaneh Sangpour for valuable comments and critical review of the manuscript.

References

[1] S. Pushpakanth, B. Srinivasan, B. Sreedhar, T.P. Sastry, An in situ approach to prepare nanorods of titania–hydroxyapatite (TiO_2–HAp) nanocomposite by microwave hydrothermal technique, Materials Chemistry and Physics 107 (2008) 492–498.

[2] S. Nath, K. Biswas, B. Basu, Phase stability and microstructure development in hydroxyapatite–mullite system, Scripta Materialia 58 (2008) 1054–1057.

[3] Z. Xihua, L. Changxia, L. Musen, B. Yunqiang, S. Junlong, Fabrication of hydroxyapatite/diopside/alumina composites by hot-press sintering process, Ceramics International 35 (2008) 1969–1973.

[4] X. Miao, Y. Hu, J. Liu, X. Huang, Hydroxyapatite coating on porous zirconia, Materials Science Engineering C 27 (2007) 257–261.

[5] D.J. Curran, T.J. Fleming, M.R. Towler, S. Hampshire, Mechanical parameters of strontium doped hydroxyapatite sintered using microwave and conventional methods, Journal of the Mechanical Behavior of Biomedical Materials 4 (2011) 2063–2073.

[6] O. Prokopiev, I. Sevostianov, Dependence of the mechanical properties of sintered hydroxyapatite on the sintering temperature, Materials Science Engineering A431 (2006) 218–227.

[7] L. He, O.C. Standard, T.T.Y. Huang, B.A. Latella, M.V. Swain, Mechanical behaviour of porous hydroxyapatite, Acta Biomaterialia 4 (2008) 577–586.

[8] Z. Zyman, I. Ivanov, D. Rochmistrov, V. Glushko, N. Tkachenko, S. Kijko, Sintering peculiarities for hydroxyapatite with different degrees of crystallinity, Journal of Biomedical Materials Research A54 (2001) 256–263.

[9] I. Mobasherpour, M.S. Hashjin, S.S.R. Toosi, R.D. Kamachali, Effect of the addition ZrO_2–Al_2O_3 on nanocrystalline hydroxyapatite bending strength and fracture toughness, Ceramics International 35 (2009) 1569–1574.

[10] A. Chiba, S. Kimura, K. Raghukandan, Y. Morizono, Effect of alumina addition on hydroxyapatite biocomposites fabricated by underwater-shock compaction, Materials Science Engineering A350 (2003) 179–183.

[11] W. Que, K.A. Khor, J.L. Xu, L.G. Yu, Hydroxyapatite/titanianano composites derived by combining high-energy ball milling with spark plasma sintering processes, Journal of European Ceramic Society 28 (2008) 3083–3090.

[12] A.A. Chaudhry, H. Yan, K. Gong, F. Inam, G. Viola, M.J. Reece, J.B.M. Goodall, I.U. Rehman, F.K. McNeil-Watson, J.C.W. Corbett, J.C. Knowles, J.A. Darr, High-strength nanograined and translucent hydroxyapatite monoliths via continuous hydrothermal synthesis and optimized spark plasma sintering, Acta Biomaterialia 7 (2011) 791–199.

[13] D. Verma, K. Katti, D. Katti, Bioactivity in in situ hydroxyapatite–polycaprolactone composites, Journal of Biomedical Materials Research A78 (2006) 772–780.

[14] M. Wang, Developing bioactive composite materials for tissue replacement, Biomaterials 24 (2003) 2133–2151.

[15] B. Viswanath, N. Ravishankar, Interfacial reactions in hydroxyapatite/alumina nanocomposites, Scripta Materialia 55 (2006) 863–866.

[16] G. Pezzotti, S. Sakakura, Study of the toughening mechanisms in bone and biomimetic hydroxyapatite materials using Raman microprobe spectroscopy, Journal of Biomedical Materials Research A65 (2003) 229–236.

[17] M.A. Meyers, A. Mishra, D.J. Benson, Mechanical properties of nanocrystalline materials, Progress in Materials Science 51 (2006) 427–556.

[18] Y. Han, S. Li, X. Wang, X. Chen, Synthesis and sintering of nanocrystalline hydroxyapatite powders by citric acid sol–gel combustion method, Materials Research Bulletin 39 (2004) 25–32.

[19] A. Eskandari, M. Aminzare, Z. Razavi hesabi, S.H. Aboutalebi, S.K. Sadrnezhaad, Effect of high energy ball milling on compressibility and sintering behaviorof alumina nanoparticles, Ceramics International 38 (2012) 2627–2632.

[20] A. Eskandari, M. Aminzare, H. Hassani, M.H. Baroonian, S. Hesaraki, S.K. Sadrnezhaad, Densification behavior and mechanical properties of biomimetic apatite nanocrystals, Current Nanoscience 7 (2011) 776–780.

[21] F. Golestani-fard, M. Mazaheri, M. Aminzare, T. Ebadzadeh, Microstructural evolution of a commercial ultrafine alumina powder densified by different methods, Journal of the European Ceramic Society 31 (2011) 2593–2599.

[22] S. Hesaraki, R. Nemati, Cephalexin-loaded injectable macroporous calcium phosphate bone cement, Journal of Biomedical Materials Research Part B(Applied Biomaterials) 89 (2009) 342–352.

[23] C. Kothapalli, M. Wei, A. Vasiliev, M.T. Shaw, Influence of temperature and concentration on the sintering behavior and mechanical properties of hydroxyapatite, Acta Materialia 52 (2004) 5655–5663.

[24] N.Y. Mostafa, Characterization, thermal stability and sintering of hydroxyapatite powders prepared by different routes, Materials Chemistry and Physics 94 (2005) 333–341.

[25] K. Khalil, S. Kima, H. Kim, Consolidation and mechanical properties of nanostructured hydroxyapatite–(ZrO_2 + 3 mol% Y_2O_3) bioceramics by high-frequency induction heat sintering, Materials and Science Engineering A456 (2007) 368–372.

[26] M. Mazaheri, Z.R. Hesabi, S.K. Sadrnezhaad, Two-step sintering of titanianoceramics assisted by anatase-to-rutile phase transformation, Scripta Materialia 59 (2008) 139–142.

[27] M.A. Auger, B. Savoini, A. Muñoz, T. Leguey, M.A. Monge, R. Pareja, J. Victoria, Mechanical characteristics of porous hydroxyapatite/oxide composites produced by post-sintering hot isostatic pressing, Ceramics International 35 (2009) 2373–2380.